Investigation of Motorcycle Handle Vibration Attenuation Using a Suspended Handlebar With Different Rubber Mount Characteristics

Nabil Mohamad Usamah, Ahmad Zhafran Ahmad Mazlan and Zaidi Mohd Ripin

TheVibrationLab, School of Mechanical Engineering, Universiti Sains Malaysia, 14300 Nibong Tebal, Pulau Pinang, Malaysia. E-mail: zhafran@usm.my

(Received 25 February 2022; accepted 15 June 2022)

Motorcycle riders are exposed to prolonged hand-transmitted vibration that can lead to hand numbness and trembling and, in extreme cases, disorders such as the Hand-arm Vibration syndrome (HAVs). The vibration of a motorcycle handle is the result of two major excitation forces, namely the engine vibration and the road-tire vibration. Operating the engine throttle control requires the rider to grip and twist the throttle handle which in turn provides a good vibration transmission path from the handle to the hand. The on-road measurement of hand-arm vibration (HAV) in a rider of an underbone single-cylinder motorcycle show a relatively high value of HAV, with a_{hv} of 8.28 m/s^2. One feasible solution is to attenuate the handlebar vibration transmissibility, by using rubber mounts to create a suspended handlebar. In this study, based on Experimental Modal Analysis (EMA), a hand gripped modal model of the handlebar is developed, and the evaluation is done on the frequency responses of different handlebar designs. The selection criterion is based on the frequency response function (FRF) synthesis index (area under curve) and in this work the area under FRF curve is taken for frequency range of 0–200 Hz based on the HAV system. Order analysis of the handle vibration showed higher acceleration level in the z-axis (vertical) compared to the y-axis (horizontal) and for the on-road testing produces, much higher vibration level is determined compared to engine-related vibration due to the tire-road interaction. The suspended handlebar with the best performance is selected for actual on-the-road test, and the result shows a lower a_{hv} value of 4.08 m/s^2 (51 % reduction), which significantly increases the vibration exposure limit value (EAV) time from 44 minutes to 3 hours.

1. INTRODUCTION

Motorcycles and scooters are the popular transportation mode, particularly in Southeast Asia, due to the underdeveloped public transportation system and traffic congestion. In 2020, the number of motorcycles sold in ASEAN region was 3.23 million units.[1] Riding a motorcycle is physically and mentally demanding, and fatigue can easily set in, with symptoms of rider fatigue including joint and muscle stiffness, pain or weakness in hands and feet, loss of concentration, as well as slow or impaired judgment and reactions.[2,3] The vibration transmitted from the motorcycle handlebar can, in certain cases, exceed the limit set by the European Directive (2002/44/EC). Methods must be found to reduce vibration if the vibration exposure surpasses the action limit value of 2.5 m/s^2. The Directive also requires the vibration exposure remain below 5.0 m/s^2. The International Standard ISO 5349[4,5] indicates that a person exposed to vibration at the vibration exposure limit value (ELV) and the vibration action limit value (EAV) has a 10 % chance of developing finger blanching after 5.8 years and 12 years of vibration exposure, respectively.

The vibration of the motorcycle handle has been reported to be in the range of 2.2 m/s^2 to 4.9 m/s^2 for traffic police motorcycle riders,[6] from 3.82 m/s^2 to 9.77 m/s^2 for motorcycle cross riders[7] and from 2.0 m/s^2 to 6.4 m/s^2 for ten test subjects in controlled testing track and riding speed.[8] At the lower end of the frequency spectrum, anti-vibration gloves have proven to be ineffective, especially at lower acceleration values.[9] The prevalence of finger blanching is 4.2 % among police traffic motorcyclists in Japan,[6] indicating that the vibration transmitted to the hand poses serious long-term health risks. The health risks of vibration to the hand are well documented.[10] These include vascular, musculoskeletal, and neurological disorders. Another negative effect of motorcycle handle vibration is the rider discomfort. This is usually self-reported, and many survey-based studies have confirmed the influence of vibration on the rider comfort. One study showed that more than 50 % of respondents reported discomfort in the hand and the arm.[11] Motorcycle ride has always been accompanied by vibration, which has unpleasant effects on both the rider and the pillion rider.[12] A survey of one hundred riders indicated that most of the respondents reported feeling vibration at the handlebar and at the footrest.[13] A study of 884 respondents shows that musculoskeletal disorders are prevalent among occupational motorcyclists; however, the study does not cover the direct effects of handle vibration on the riders.[14]

Numerous attempts have been made to overcome hand and arm vibrations experienced by motorcyclists. Using a tuned mass damper (TMD) on the motorcycle handlebar can reduced the performance index by 22 %, indicating a reduction in the vibration energy transfer from the source to the handlebar.[15] The same technique is also used which resulting a vibration reduction from 23 % to 66 %. Both cases suffered from a smaller frequency bandwidth application which requires specific tuning for a particular case 16. A particle damper was installed on the handlebar in some studies and able to alleviate the Hand-arm Vibration syndrome (HAVs) by reducing the vibration response by 50 %.[17] A dynamic vibration absorber (DVA) has also proven to effectively attenuate the motorcycle handlebar vibration peaks by up to 68 %. However, the approach only be implemented in a single focused dominant axis.[18] In other study, a suspended handlebar is applied on a motorcycle while riding and resulting of 79 % hand-arm weighted RMS acceleration reduction. However, the study is focused on a dynamic properties simulation to increase the efficacy of the design without the effect of hand grip on the handlebar.[19] In other types of handheld machinery, the use of rubber mounts on a suspended handle of a petrol grass trimmer successfully reduced the total hand-arm vibration value by 76 %.[20]

The aim of the study presented here is to study and reduce the vibration transmission from the motorcycle handlebar to the rider hands, by installing an optimized suspended handlebar design. The dynamic characteristics of the handles while gripped by the rider are derived from Experimental Modal Analysis (EMA) results.[21] A hand gripped handlebar modal model is then developed in MATLAB-Simulink and used to evaluate the different suspended handlebar designs (different rubber mounts dynamic properties) and to identify the best attenuation performance. The final vibration and efficacy are determined by measuring the hand-arm vibration (HAV) values during on-road hand acceleration spectra measurement.

2. THEORETICAL DEVELOPMENT

The vibration level of a suspended handlebar can be evaluated qualitatively, based on the structure's response, $x(\omega)$. In this section, we introduce the different values of damping, C, and stiffness, K, representing the characteristics of the rubber mounts.[22,23] The equation of motion for the original handlebar is shown as:

$$M\ddot{x}_0 + C\dot{x}_0 + Kx_0 = f(\omega); \tag{1}$$

where $C = \alpha M + \beta K$ was the assumed proportional viscous damping. For the modified system, assuming that $\Delta C = \alpha\Delta M + \beta\Delta K$, to maintain the proportional damping. The equation of motion for the suspended handlebar was expressed as:

$$(M + \Delta M)\ddot{u} + (C + \Delta C)\dot{u} + (K + \Delta K)u = f(\omega). \tag{2}$$

The impedance-like matrix of the original structure, $z_0(\omega)$ was derived from the frequency response function (FRF) matrix of the original $x_0(\omega)$ was:

$$x_0(\omega) = H_0(\omega)f(\omega); \tag{3}$$

$$[z_0(\omega)]^{-1} = H_0(\omega). \tag{4}$$

The dynamic stiffness $\Delta Z(\omega)$ was expressed as:

$$\Delta Z(\omega) = \Delta K + j\omega\Delta C - \omega^2\Delta M; \tag{5}$$

thus, the suspended handlebar's response, $x(\omega)$ and the FRF matrix of this modified system, $H(\omega)$ can be obtained as shown below:

$$x(\omega) = H(\omega)f(\omega); \tag{6}$$

$$H(\omega) = [I + H_0(\omega)\Delta Z(\omega)]^{-1}H_0(\omega); \tag{7}$$

where $f(\omega)$ was the external excitation and I was the identity matrix. The response, $x(\omega)$ directly correlates with the acceleration, $\ddot{x}(\omega)$.

To measure the efficacy of the technique, the acceleration in the frequency spectrum was integrated to calculate the area under the graph known as synthesis index shown in Eq. (8). Higher synthesis index indicating higher vibration energy was transferred to the structure.[15]

$$\text{Synthesis index} = \int_{0Hz}^{200Hz} a_h d\omega; \tag{8}$$

where a_h was the value of root mean square (RMS) acceleration in m/s^2, and ω was the frequency (for hand arm vibration $\omega_0 = 200Hz$)

Based on ISO 5349-1 and ISO 5349-2, the total HAV value was calculated using Eq. (9) and Eq. (10) for comparison.[4,5]

$$a_{hw} = \sqrt{\sum_j (W_{hj}a_{hj})^2}; \tag{9}$$

$$a_{hv} = \sqrt{a_{hwx}^2 + a_{hwy}^2 + a_{hwz}^2}; \tag{10}$$

where for Eq. (9), W_{hj} was the weightage multiplication factor for the frequency band, j, a_{hj} was the RMS of the acceleration, and a_{hw} was the frequency of the weighted RMS acceleration on the frequency band. Meanwhile, for Eq. (10), a_{hwx}, a_{hwy}, and a_{hwz} were the frequency weighted RMS acceleration values on the frequency band for the $x-$, $y-$, and $z-$axis, respectively. Finally, a_{hv} was the total HAV value.

3. METHODOLOGY

An underbone motorcycle with a 70-cc single-cylinder, four-stroke engine was used in this analysis. The overall methodology covers four important phases, and detailed explanations of each measurement phase are given in the next sub-chapters.

3.1. Experimental Modal Analysis With Different Rubber Mounts

The dimensions of motorcycle handlebars were measured and modelled in LMS Test Lab, using the geometry workbench. Figure 1 a and 1 b show the 3D model of motorcycle stock and suspended handlebar. The node's location was measured and labeled with stickers before performing the EMA, as shown in Fig. 1 d. EMA was carried out for the motorcycle handlebar, for both the free-free condition and the condition where the rider's hand was gripping the handle, to quantify the effect of the grip. A small lightweight accelerometer (Dytran 3055B2T) was used to measure the vibration response, while an impact hammer (Krisler 9724A5000) excites the motorcycle handlebar. Both were connected to the 8-channel LMS SCADAS Mobile. The accelerometers are firstly calibrated,

Table 1. Rubber mount dimensions.

Rubber mount type	a (mm) rubber	b (mm) rubber	c (mm) steel	d (mm) steel	e (mm) rubber	f (mm) rubber	g (mm) rubber
A	46.0	14.0	13.0	6.0	15.0	22.0	3.0
B	42.2	22.2	10.0	6.0	24.5	N/A	N/A
C	40.4	13.0	10.0	6.0	15.0	22.0	3.7
D	48.0	14.0	14.0	5.0	15.0	21.0	3.0

using the calibration exciter (B&K 4294). From the EMA, the modal properties of the handles were derived, by scaling the mode shapes to the unit modal mass.[24] A sine-swept vibration source, with a frequency range from 0 Hz to 200 Hz, and the amplitude of 10 m/s^2, was applied to the base. Each handle acceleration response was compared, to evaluate the effectiveness of the suspended handles. The frequency responses of the stock handlebar and the suspended handlebar models, with four different rubber mount dimensions that made of from natural rubber and steel (Cross section shown in Fig. 1 c and detail dimension in Table 1), were calculated and compared, to find the best design with the lowest handlebar vibration level. The dynamic characteristics of the suspended handlebars, which were dependent on the dynamic characteristics of the rubber mounts, obtained from the EMA, are listed in Table 4 of Appendix section.[20]

3.2. In-Lab Testing

For the in-lab testing, the HAV level was measured with the engine running and the transmission in the third gear at which the cruising speed was achieved. The motorcycle was kept upright on its centre double stand, and the rear wheel was allowed to rotate. Figure 1 e shows the experimental setup for the in-lab testing. The measurement instruments included two accelerometers (Dytran 3055B2T) for the $z-$ and the $y-$axes on the rider's right hand, a tachometer (Optel-Thevon 152), a calibrator (B&K 4294), data acquisition software (LMS Test Express), data acquisition hardware (LMS SCADAS Mobile), and a portable workstation.

3.3. On-Road Testing

Figure 1 f shows the experimental setup for the on-road testing. It was carried out on a straight, flat asphalt road surface, over a period of 120 seconds. Accelerometers were located on the rider's left hand, to measure the HAV. The tachometer was mounted on the motorcycle's engine chassis, to measure the engine speed. The sensors were connected to the LMS SCADAS Mobile using the LMS Test Express software on a portable computer for the data acquisition system. The test was repeated for the selected suspended motorcycle handlebar, to evaluate the effectiveness of the vibration attenuation. The method adopted here was to carry out the order-analysis within the speed range and for each speed data point, the value of a_{hv} for the whole sample (speed independent and time-averaging) during the measurement process can be obtained. With this technique, we can plot the a_{hv} as a function of speed and this method has not been reported anywhere in the literature.

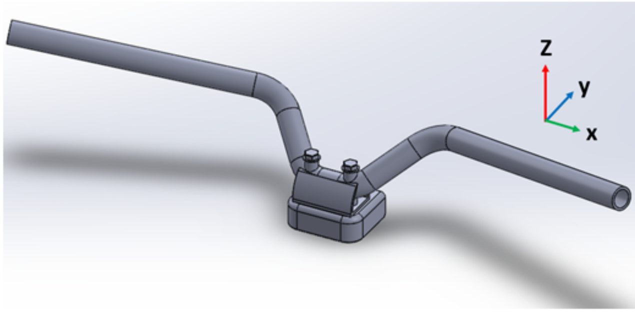

(a) Stock handlebar 3D design.

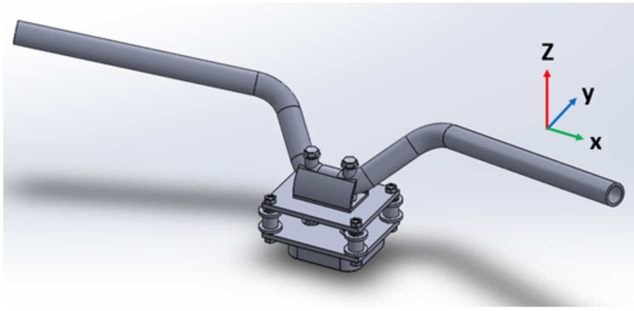

(b) Suspended handlebar 3D design.

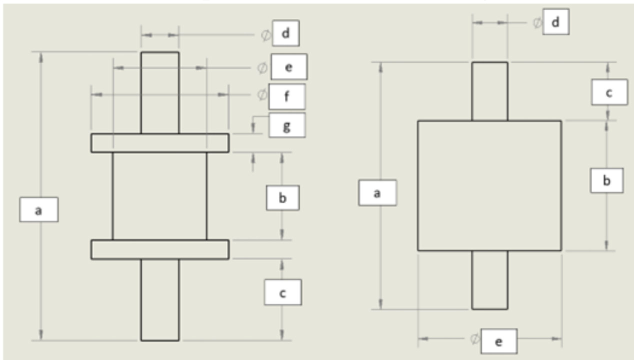

(c) Rubber mounting dimension diagram.

Figure 1. (a) - (c) Experimental setup and pictures.[19]

4. RESULTS AND DISCUSSION

4.1. EMA Results Of The Handlebar

Figure 2 shows the FRF curves for the stock handlebar, both on its own and when subjected to the hand grip for the y- and z-axes. Within the frequency range of 0 Hz to 200 Hz, which is the interventional frequency range used to address the HAV, the FRF values for the z-axis (vertical) are generally much higher than those for the $y-$axis (horizontal). The presence of the rider hand on the handlebar increases the damping and reduces the resonance peak. For natural frequencies exceeding 200 Hz, the amplitude peaks are reduced by about 70 %. In contrast, at natural frequencies below 200 Hz, the amplitude peaks are reduced by 90 %. These data show that the hand grip increases the handlebar damping significantly, particularly at lower frequencies. Given the presence of the hand gripping effect, the handlebar must now be considered a highly damped system. The FRF curves for the hand-gripped handlebar for the $y-$ and $z-$axes do not show clear peaks as displayed, when compared with the handle-only FRF curve. The highly damped hand-handle system may indicate that narrow-band attenuation, such as the tuned vibration absorber (TVA), may not be

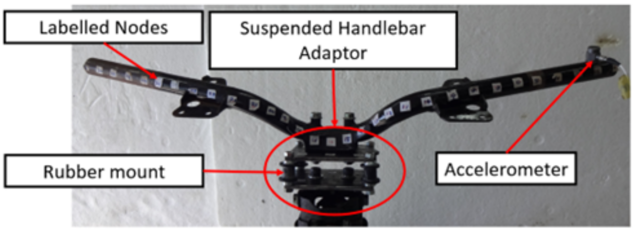

(d) EMA setup.

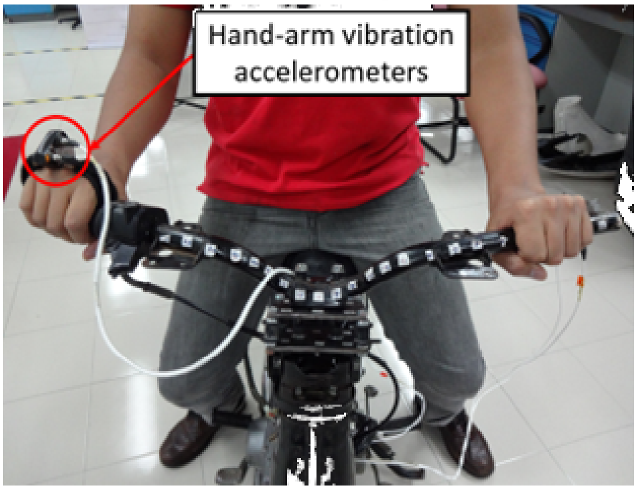

(e) In-lab measurement.

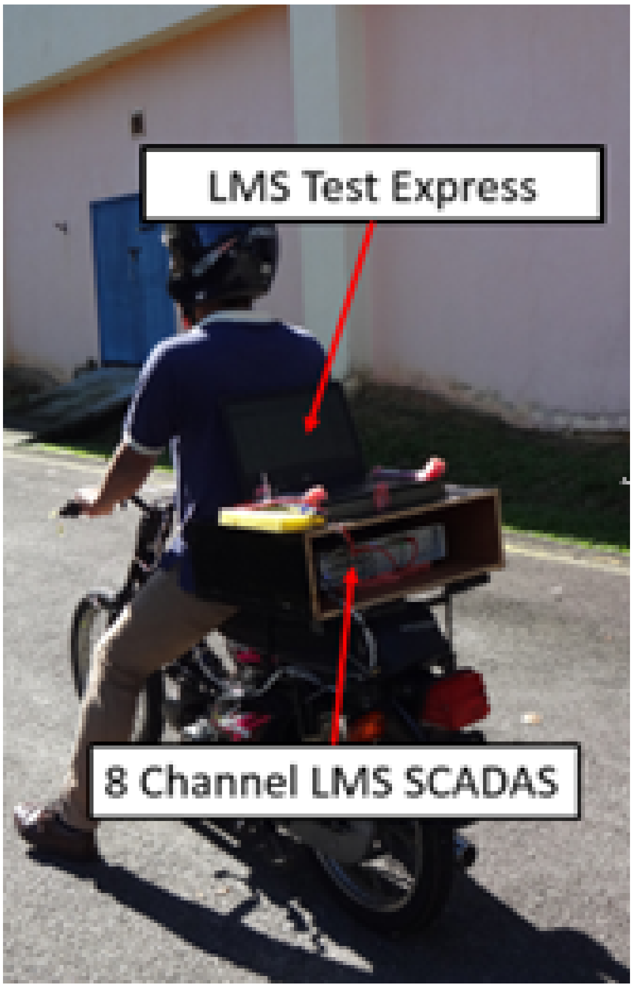

(f) On-road measurement.

Figure 1. cont. (d) - (f) Experimental setup and pictures.[19]

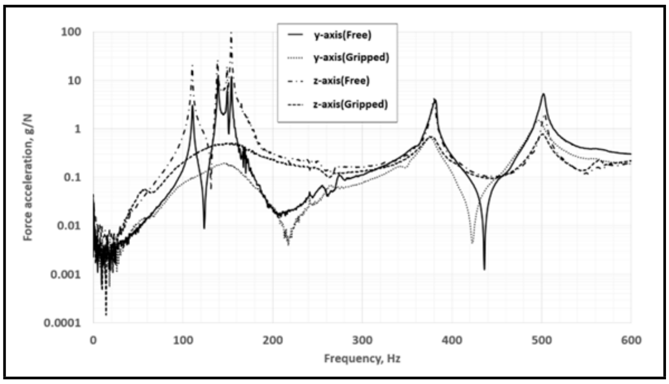

Figure 2. FRF curve for the stock handlebar, with and without rider's hands gripping the end of the handlebar.

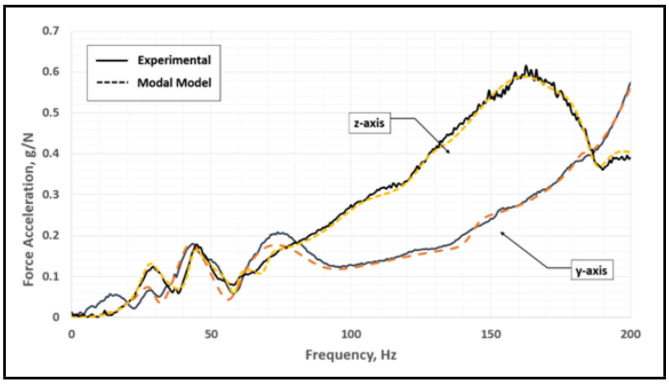

Figure 3. Motorcycle stock handlebar raw FRF curves and modal model for the $y-$ and $z-$axes.

effective. Due to these differences in the level of dynamic response between the gripped and the hand-free handlebar, the hand-gripped handlebar FRF is selected for the modal model development. All the previous studies have downplayed this effect.[15] In this work, however, the modal model includes the hand grip effect, as it is important to keep the model as close as possible to the actual conditions.

4.2. Handlebar Modal Models Development And Evaluation

Three dominant modes are selected from the modal model FRF, to be used as handlebar modal models. For the stock handlebar (HS), the modes at the frequencies of 41.6 Hz, 82.2 Hz, and 183.0 Hz (Table 4 in Appendix) are chosen to represent the handle-hand system, as these are the only modes below 200 Hz that are considered important in the HAV system. All the modes are scaled to the unit modal mass, set to unity, and normalized.[24] The selected modes (Mode 1, 2 and 3), as well as the scaled stiffness and the damping coefficients, are listed in Table 4 of Appendix section. The data obtained from the EMA are used to derive the modal parameters for the modal model. To check the model validity, the model FRF is compared with the experimental FRF, as shown in Fig. 3 for the stock handlebar. In this figure, the FRF curves for the models in both $y-$ and $z-$axes matched the experimental values, with a correlation value of more than 95 % for both axes.

Table 2. Motorcycle handlebars non-weighted and weighted RMS synthesis index.

RMS Synthesis Index	Stock (m/s^2)	Design A (m/s^2)	Design B (m/s^2)	Design C (m/s^2)	Design D (m/s^2)
Handlebar (Non-weighted)	67.255	142.500	56.489	93.626	57.993
Handlebar (Weighted)	25.874	33.139	22.081	29.456	22.926

4.3. RMS Synthesis Index Evaluation Of The Handlebar Models

A sine-swept signal was applied at frequencies ranging from 0.1 Hz to 200 Hz, with a constant amplitude of 10 m/s^2, to obtain the model acceleration response, and to evaluate the performance of the four suspended handles. Figure 4 a shows the model acceleration frequency response in the $y-$axis (horizontal) for the different mounts. For the stock handle, the peak response is 0.4 g at the frequency of 46 Hz, and each handlebar with rubber mounts has a different natural frequency and, at frequencies between 40 Hz to 65 Hz, handlebar designs B and D demonstrate lower acceleration responses than the stock handlebar. Figure 4 b shows the model's response in the $z-$axis (vertical). The stock handlebar has a peak response of 0.46 g at 24 Hz. Each suspended handlebar design produces a different response, and at frequencies range of 20 to 75 Hz, handlebar designs B and D resulted in lower acceleration responses than the stock handlebar. Therefore, handlebar designs B and D can be used for the attenuation of the handlebar vibration. This is supported by the RMS synthesis index values shown in Table 2, whereby both designs B and D produced the lowest RMS synthesis index for weighted and non-weighted handlebars. Based on both RMS synthesis index evaluations, design B and D handlebar gives the best responses, however all the handlebars will be further analyzed in the subsequent of on-road hand-arm acceleration spectra testing.

4.4. In-Lab Hand Acceleration Spectra Results

Figure 5 a and 5 b show the hand acceleration spectra of the stock handlebar for in-lab testing for both the $y-$ and $z-$axes. For the $z-$axis, the highest acceleration recorded is 0.38 g at 101 Hz with engine speed of 4000 rpm while for the $y-$axis, the highest acceleration is 0.11 g at 100 Hz with the same engine speed. It is clearly shown that the engine induced vibrations are dominant in the $z-$axis indicated by the higher vibration compared to $y-$axis. Both figures show similar pattern, with the peak moving toward higher frequency as the engine speed increases. It is also clear that the handle vibration spectrum is not directly or linearly related to the engine speed indicating that, it is order independent.

Figure 7 b shows a graph of HAV values, a_{hv}, against the engine speed measured at the stock handlebar, obtained from in-lab and on-road vibration testing. The in-lab test results show that the a_{hv} value starts out at 4.0 m/s^2 when the engine speed is 2000 rpm and gradually increases with the engine speed, to 5.5 m/s^2 at the maximum engine speed of 4000 rpm. For the on-road testing, at the initial engine speed of 2000 rpm, $a_{hv} = 5.6$ m/s^2, and remains constant until the speed reaches 2700 rpm. After this, the a_{hv} value generally increases with the speed. At the maximum speed of 4000 rpm,

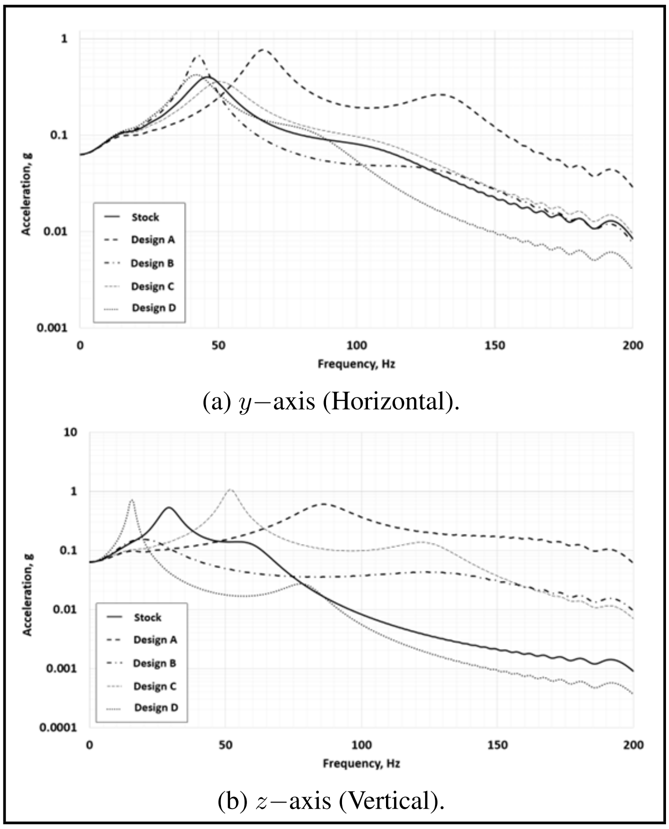

(a) $y-$axis (Horizontal).

(b) $z-$axis (Vertical).

Figure 4. Acceleration response spectra of handlebar models in (a) $y-$ and (b) $z-$axes.

$a_{hv} = 14.4$ m/s^2, which is much higher than the value obtained from the in-lab measurement. Within the engine cruising speed range, the average HAV value obtained from the on-road testing is 8.18 m/s^2 and, based on the European Directive (2002/44/EC), it would take 45 minutes to reach the EAV, and 2 hours and 59 minutes to reach the ELV at that rate. Meanwhile, the in-lab testing produces an average hand-arm vibration value of 4.74 m/s^2, and it would take 2 hours and 14 minutes to reach the EAV, and 8 hours and 54 minutes to reach the ELV at this rate. The differences between the on-road and the in-lab vibration shows the strong effect of the road-tire vibration on the motorcycle handlebar during operation. Both results indicate the need for intervention, especially for an extended motorcycle ride.

4.5. On-Road Hand Acceleration Spectra Results

For the on-road testing, the acceleration level is presented in the combined frequency-and-engine speed form, to identify engine speed related vibration (also known as the waterfall plot). Figure 6 a shows the acceleration reading on the hand in $y-$axis for the frequency range from 0 to 200 Hz and the engine speed ranging from 2000 rpm to 4000 rpm, on a typical weathered road. As the figure indicates, the acceleration response is high at frequencies below 75 Hz. The peak values are at 0.4–0.6 g, depending on the frequency. Also, there is no clear speed-dependent response (order effect). This shows that the engine vibration effect on the handle is relatively small and overwhelmed by the road-tire vibration signals. At speeds ranging from 2000 rpm to 2600 rpm, the

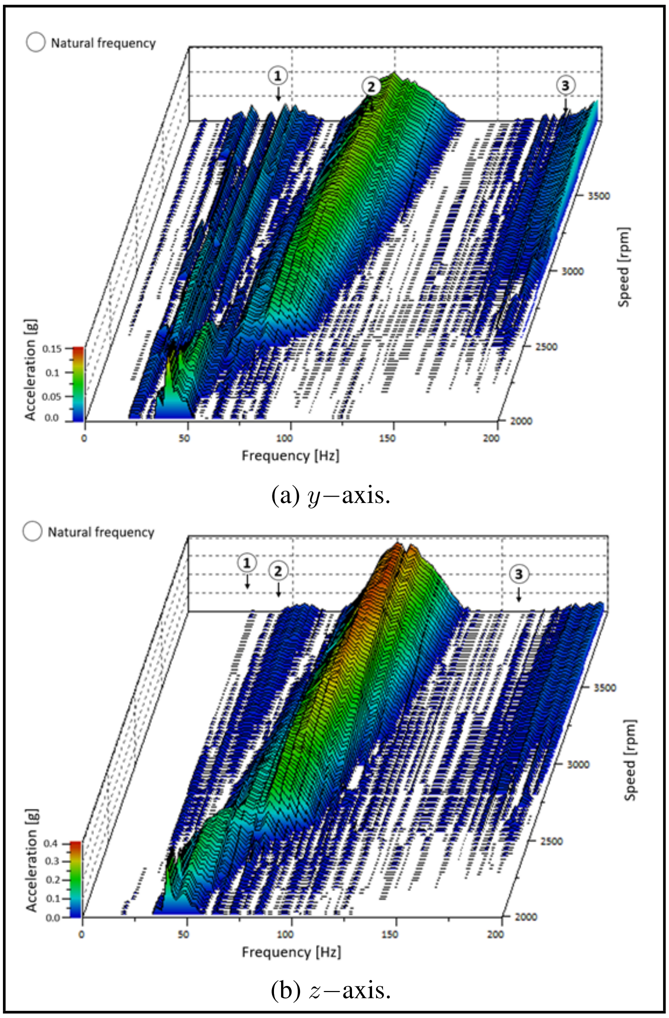

(a) $y-$axis.

(b) $z-$axis.

Figure 5. Hand acceleration spectra for the stock handlebar during in-lab testing at various engine speeds in (a) $y-$ and (b) $z-$axes.

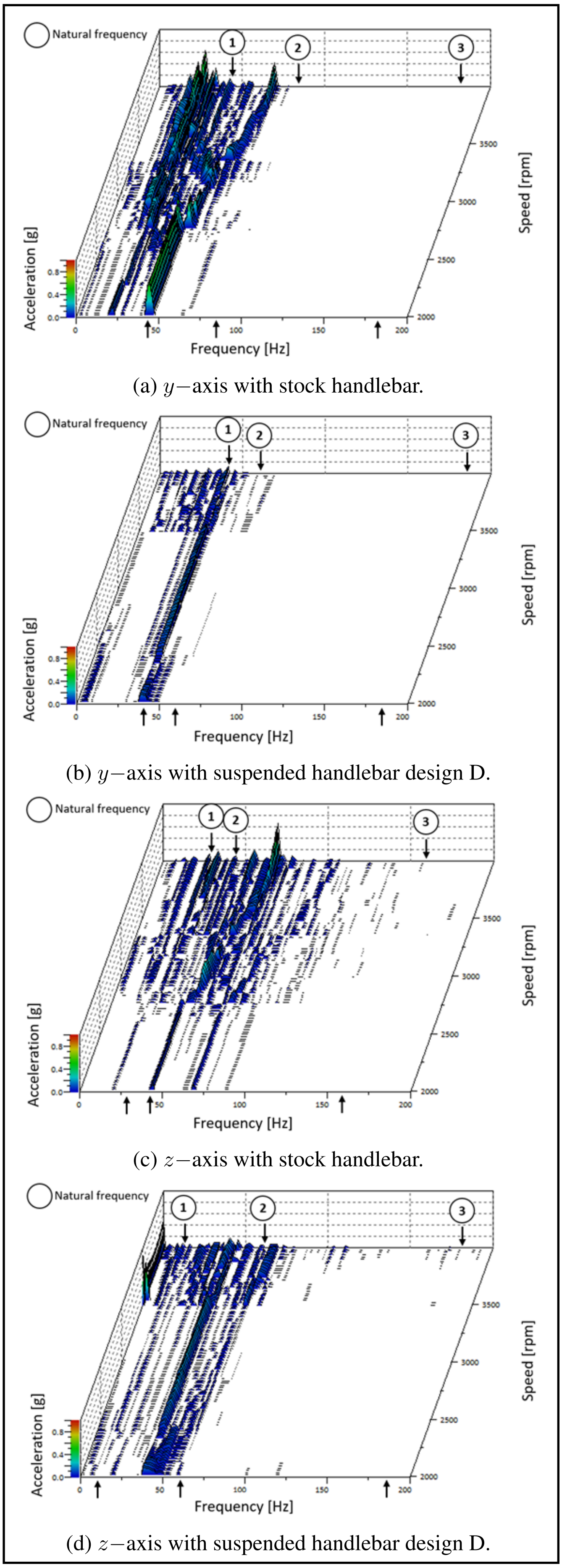

(a) $y-$axis with stock handlebar.

(b) $y-$axis with suspended handlebar design D.

(c) $z-$axis with stock handlebar.

(d) $z-$axis with suspended handlebar design D.

Figure 6. Hand acceleration spectra for the stock handlebar (a) $y-$, (c) $z-$axes and suspended handlebar design D (b) $y-$, (d) $z-$axes at various engine speeds.

peaks reach nearly equal heights as they cluster around the first frequency mode at approximately 41.60 Hz. This speed-independent, constant-frequency response indicates that the vibration here is resonance-related. The speed range from 2600 rpm to 4000 rpm shows another ridge at the frequency of 54 Hz, and the amplitude increases with the engine speed as the engine speed is approaching 4000 rpm. The speed- and frequency-dependent nature of the peaks can be attributed to the typical first-order engine-related vibration sources, primarily the engine unbalance. Meanwhile, the peaks within this speed range cluster around frequencies ranging from approximately 20 Hz to 45 Hz at speeds ranging from 2500 rpm to 4000 rpm, which are attributed to the road-tire interaction. As Fig. 6 b demonstrates, installing a design D suspended handlebar alters the handlebar's dynamic characteristics in y-axis, where the highest peaks within the speed range from 1500 rpm to 4000 rpm cluster around the first mode frequency of 39.51 Hz. With the introduction of the rubber mount D in the suspended handlebar, in this case, the peaks within the speed range from 1500 rpm to 4000 rpm cluster around the handlebar's first mode of natural frequency, and the vibration level is reduced to below 0.2 g. The vibration amplitude of the engine-speed- and frequency-dependent peaks is effectively reduced in the design D suspended handlebar case, especially in the speed range from 3000 rpm to 3600 rpm, as it is within the

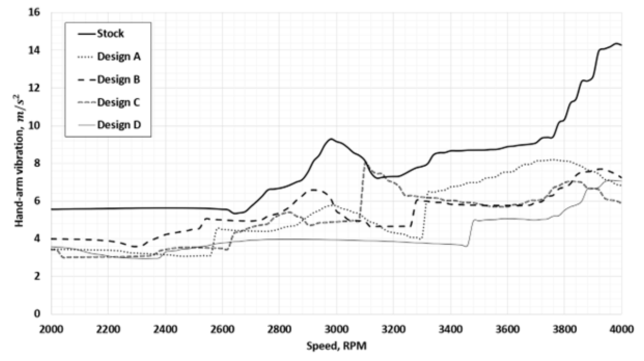

(a) Comparison of different designs for on-road HAV acceleration values.

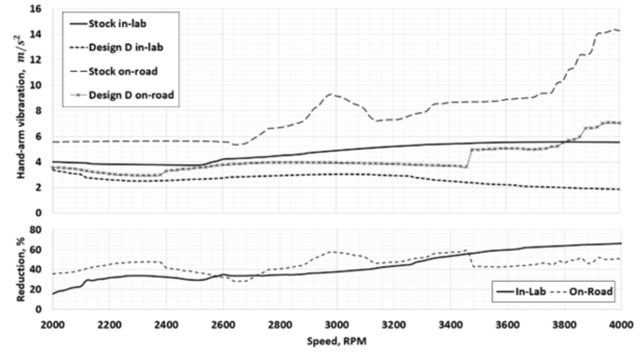

(b) Detailed in-lab and on-road HAV acceleration values and percentage of reduction (Design D).

Figure 7. (a) – (b) Overall HAV acceleration values and reduction percentage against engine speed.

cruising speed range of the motorcycle at 50 – 60 km/h.

For the $z-$axis response in Fig. 6 c, the stock handlebar vibration displays its first cluster of peaks within the speed range from 2650 rpm to 4000 rpm, with the frequencies clustering around 27.42 Hz, which coincides with the first mode in the $z-$axis. At speeds ranging between 1500 rpm and 2650 rpm, the peaks cluster around the frequency of 43.24 Hz, which coincides with the second mode for the $z-$axis. At speeds ranging from 2650 rpm to 4000 rpm, the peak linearly increases as the engine speed increases to 4000 rpm. At the top engine speed of 4000 rpm, the peak value of the acceleration reaches 0.6 g at 75 Hz. Based on the results for both the $y-$ and the $z-$axes, the stock handlebar suffers from the large vibration amplitude at the natural frequencies. For the suspended handlebar design D response in the $z-$axis shown in Fig. 6 d, the smaller peaks cluster is obtained around frequencies of 13.31 Hz and 63.36 Hz. Higher peaks are shown to constantly cluster around a single frequency of 40 Hz. The engine-speed-and frequency-dependent peaks are effectively reduced by the proposed suspended handlebar. The data for the on-the road test verify the effectiveness of the suspended handlebars in reducing the HAV.

4.6. HAV α_{hv} Analysis For Handlebars

To measure the efficacy of the approach, the HAV values for the handlebars, a_{hv}, in both the $y-$ and the $z-$axes, are calculated for each speed condition. Figure 7 a shows the a_{hv} values for the stock and the suspended handlebar A, B, C, and D during the on-road testing. For the whole engine speed range of 2000 rpm to 4000 rpm, the stock handlebar has the highest a_{hv} value compared to the suspended handlebars, except for the design C in the speed range of 3100 rpm to 3170 rpm. From the figure, it shows that the proposed suspended handlebar technique is effective in reducing the HAV. Focusing on the cruising speed range of 3000 rpm to 3600 rpm, design D shows the lowest average a_{hv} values compared to the other suspended handlebar designs.

Table 3. Motorcycle handlebar average cruising speed HAV value.

Average HAV (cruising)	Stock (m/s^2)	Design A (m/s^2)	Design B (m/s^2)	Design C (m/s^2)	Design D (m/s^2)
Handlebar	8.276	5.823	5.398	6.135	4.082

Figure 7 b shows the a_{hv} values for the stock and the design D suspended handlebar in greater detail, and their reduction percentages at engine speeds in the range from 2000 rpm to 4000 rpm. The figure also indicates that the a_{hv} values for the stock handlebar are higher than those for suspended handlebar design D during on-the-road testing at speeds ranging from 2000 rpm to 4000 rpm. The vibration reduction percentage is between 20 – 60 % for the in-lab testing, and for the on-road testing is about 25 – 58 %. Focusing on the engine cruising speed during the on-road testing, the highest HAV values are 9.17 m/s^2 at the speed of 3000 rpm for the stock handlebar and 3.94 m/s^2 at the same speed for the design D suspended handlebar. The average HAV values for the stock and the design D suspended handlebars in the engine cruising speed range are 8.28 m/s^2 and 4.08 m/s^2, (as shown in Table 3), indicating an average HAV reduction value of 51 %. However, the highest HAV reduction value during the on-road testing is 58 %, at the engine speed of 3460 rpm. Thus, the suspended handlebar with rubber mount D directly reduces the hand-arm exposure, increasing the time it takes to reach the EAV limit from 45 minutes to 3 hours 17 minutes. The time to reach the ELV increases from 3 hours 17 minutes to 13 hours 9 minutes. The impact of the suspended handlebar is truly significant.

In this study, the effectiveness of using the suspended handlebar at reducing the vibration can be compared with that of other approaches. Passive attenuation, such as the implementation of particle dampers on the motorcycle handlebar ends, has been reported to reduce the vibration by up to 50 %.[17] However, no on-road data is provided meanwhile, installing a TMD reduces the performance index by 22 %, which is explained by the fact that a TMD exhibits a new second mode of vibration that leads to a lower vibration isolation in a wide range operating frequency.[15] The use of TMD is known to be effective, however the directional properties are not reported. It is interesting to note that Agostoni use synthesis index, which is basically the area under the FRF, and not frequency weighted.[15] Our approach here is to use the weighted a_{hv} for the selection of the suspended handle design. For each FRF of the design, both the a_{hv} and synthesis index of the acceleration response function are calculated and the values for the $y-$ and $z-$axes are shown in Fig. 8. The a_{hv} values pointed design D as the lowest vibration, whereas synthesis index pointed to design B.

A DVA used on a test motorcycle was proven to effectively attenuate the vibration peak by up to 68 % in the respective

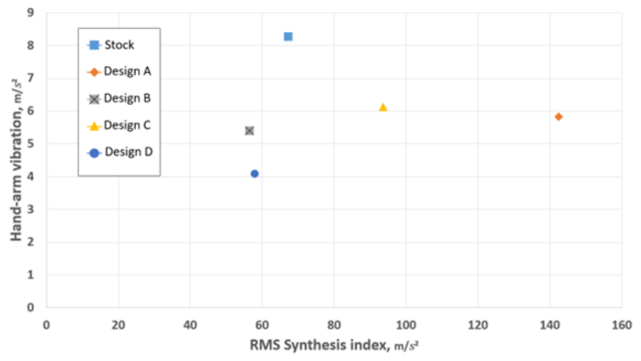

(a) HAV vs RMS synthesis index.

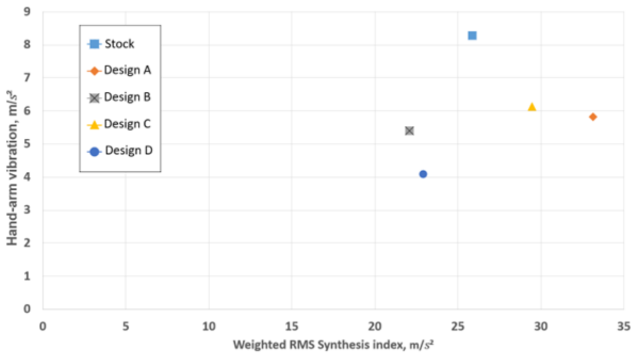

(b) HAV vs weighted RMS synthesis index.

Figure 8. (a) – (b) Motorcycle handlebars HAV versus RMS synthesis index.

axes.[18] A similar passive attenuation technique, which involved a tuning on mounting position and rubber mounts positioning for the suspended adaptor, was used on a single petrol grass trimmer, operating at a selected operating frequency, and successfully reducing the total HAV values by 76 %.[19] Tuned and specific frequency targeted approaches, such as TMD and DVA, can be ineffective for variable operating engine speed conditions. The work carried out here shows that suspended handles, based primarily on the structural dynamic alteration of damping and stiffness coefficients, are effective in wider frequency spectrum ranges, with an average HAV reduction value of 51 % at speeds ranging from 3000 rpm to 3600 rpm, and can be adopted in underbone motorcycles.

5. CONCLUSION

In this study, a suspended handle adaptor has been developed, to attenuate the motorcycle handlebar vibration transmitted to the rider. Four different suspended handlebar designs (with different rubber mount characteristics) have been developed, and their performances were compared for both in-lab and on-road testing. Based on the HAV analysis, the handlebar design D performing better than other designs. The average hand-arm weighted RMS acceleration, a_{hv}, obtained from on-road test in the cruising speed range, is reduced by 51 %, from 8.28 m/s^2 to 4.08 m/s^2, indicating the efficacy of the suspended handlebar design D. The suspended handlebar increases the time it takes to reach the EAV from 44 minutes to 197 minutes, which is well below the daily exposure time for majority riders and significantly reducing the rider's risk of the HAVs.

ACKNOWLEDGEMENTS

The authors would like to thank the Ministry of Higher Education Malaysia for Fundamental Research Grant Scheme (FRGS) with Project Code: FRGS/1/2021/TK0/USM/03/6 and Universiti Sains Malaysia (USM) grant A/C 304/PMEKANIK/6316214.

REFERENCES

1 Number of motorcycles and scooters sold in the ASEAN region 2020. Accessed May 10, 2022. https://www.statista.com/statistics/584019/asean-motorcycle-and-scooter-sales-by-country/

2 Ma, T., Williamson, T., and Friswell, R. *A pilot study of fatigue on motorcycle day trips*. Sydney-NSW Injury Risk Management Research Centre, (2003).

3 Machado, S., Hugo, Sanchez, E.G. de M., Barbosa M.A., Celeno, C., Porto, and Approbato, M.S., Comparison of quality of life and work ability of taxi and motorcycle taxi drivers: evidence from Brazil. *International journal of environmental research and public health*, **16**(4), 666, 2019. https://doi.org/10.3390/ijerph16040666

4 ISO ISO. 5349-1: *Mechanical vibration-measurement and evaluation of human exposure to hand-transmitted vibration-part 1: general requirements*. Geneva, Switzerland: International Organization for Standardization. Published online 2001.

5 ISO I. 5349-2: *Mechanical vibration- Measurement and evaluation of human exposure to hand-transmitted vibration-part 2: Practical guidance for measurement at the workplace*. Geneva, Switzerland: International Organization for Standardization. Published online 2002.

6 Mirbod, S.M., Yoshida, H., Jamali, M., Masamura, K., Inaba, R., and Iwata, H. Assessment of hand-arm vibration exposure among traffic police motorcyclists. *International Archives of occupational and Environmental health*, **70**(1), 22-28, 1997. https://doi.org/10.1007/s004200050182

7 Roseiro, L.M., Neto, M.A., Amaro, A.M., Alcobia, C. J., and Paulino. M. F. Hand-arm and whole-body vibrations induced in cross motorcycle and bicycle drivers. *International journal of industrial ergonomics*, **56**, 150-160, 2016. https://doi.org/10.1016/j.ergon.2016.10.008

8 Noh, J.M., Rezali, K.A.M., As' arry, A., and Jalil, N. A. A. Transmission of vibration from motorcycle handlebar to the hand. *Journal of the Society of Automotive Engineers Malaysia*, **1**(3), 191-197, 2017. https://doi.org/10.56381/jsaem.v1i3.64

9 Yokomori, M., Yamada, S., Nakagawa, T., and Matsumoto, T. The vibration of the handle-bars of a motorcycle in running on the paved road (author's transl). Sangyo igaku.

Japanese Journal of Industrial Health, **23**(2), 134-140, 1981. https://doi.org/10.1539/joh1959.23.134

[10] Griffin, Michael J., and John Erdreich. *Handbook of human vibration*, 2213-2213, 1991.

[11] Karuppiah, K., Salit, M.S., Ismail, M.Y., Ismail, N., and Tamrin, S. Evaluation of motorcyclist's discomfort during prolonged riding process with and without lumbar support. *Anais da Academia Brasileira de Ciências*, **84**(4), 1169-1188, 2012. https://doi.org/10.1590/S0001-37652012000400031

[12] Jeyapal, R.B. *Judging the discomfort of vibration on motorbike*. Institute of Sound and Vibration Research, University of Southampton, UK. Published online 2014.

[13] Khamis, N.K., MIsmail, F.R.B., and Tahir, N.H. Motorcycle deliveryman's perceptions on riding conditions. *Malaysian Journal of Public Health Medicine*, 63-67, 2016.

[14] Hafzi, M.M., Rohayu, S., Faradila, P.N., and Wong, S.V. Prevalence and risk factors of musculoskeletal disorders of motorcyclists. *Prevalence*, **1**, 2011.

[15] Agostoni, S., Cheli, F., Leo, E., and Pezzola, M. An innovative multi dof TMD system for motorcycle handlebars designed to reduce structural vibrations and human exposure. *Mechanical Systems and Signal Processing* **31**, 298-315, 2012. https://doi.org/10.1016/j.ymssp.2011.11.018

[16] Khune, S.S., and Bhende, A.R. Design of Motorcycle Handlebar for Reduction of Vibrations Using Tuned Mass Damper. *Advances in Mechanical Engineering*, 329-335. Springer, Singapore, 2021. https://doi.org/10.1007/978-981-15-3639-7_38

[17] Baad, S.M., Patil, R.J., and Qaimi, M.G. Hand arm vibration alleviation of motorcycle handlebar using particle damper. *Int. J. Eng. Manuf*, **7**(1), 26-40, 2017. https://doi.org/10.5815/ijem.2017.01.03

[18] Saifudin, M.I.A.M., Usamah, N.M., and Ripin, Z.M. Attenuation of Motorcycle Handle Vibration Using Dynamic Vibration Absorber. *MATEC Web of Conferences*, **217**, 01006, 2018. https://doi.org/10.1051/matecconf/201821701006

[19] Usamah, N.M., and Ripin, Z.M. Attenution of Motorcycle Handle Vibration using Suspended Handlebar. *IOP Conference Series: Materials Science and Engineering*, **815**(1), 012013, 2020. https://doi.org/10.1088/1757-899x/815/1/012013

[20] Ko, Y.H., Ean, O.L., and Ripin, Z.M. The design and development of suspended handles for reducing hand-arm vibration in petrol driven grass trimmer." *International Journal of Industrial Ergonomics*, **41**(5), 459-470, 2011. https://doi.org/10.1016/j.ergon.2011.04.004

[21] Fu Z.F., He J. *Modal Analysis*. Butterworth-Heinemann; 2001.

[22] Sestieri, A., & D'Ambrogio, W. *Encyclopedia of Vibration - Structural dynamic modifications*, 1253-1264, 2001. https://doi.org/10.1006/rwvb.2001.0100

[23] Satar, M.H.A., Nyap, W.J., and Mazlan, A.Z.A. Numerical Approach on Hybrid PID-AFC Controller using Different Intelligent Tuning Methods to Reduce the Vibration of the Suspended Handle. *International Journal of Acoustics & Vibration*, **26**(1), 28-40, 2021. https://doi.org/10.20855/ijav.2020.25.11713

[24] Richardson, M.H., and Jamestown, C. M*odal mass, stiffness and damping*. Vibrant Technology, Inc., Jamestown, CA, 1-5, 2000.

APPENDIX

Table 4. Motorcycle handlebar modes properties.

	Mode 1			Mode 2			Mode 3		
y-axis	Frequency (Hz)	Stiffness (kN/m)	Damping (Kg/s)	Frequency (Hz)	Stiffness (kN/m)	Damping (Kg/s)	Frequency (Hz)	Stiffness (kN/m)	Damping (Kg/s)
HS	41.60	69.91	79.72	82.21	276.56	197.35	183.03	1320.00	37.63
HA	62.62	157.03	94.53	100.52	400.08	69.52	153.53	930.78	29.08
HB	37.36	55.42	35.56	102.65	432.93	260.35	189.96	1420.00	14.14
HC	46.08	86.89	110.94	82.62	276.31	187.15	193.36	1490.00	239.14
HD	39.51	62.77	91.32	61.72	152.27	86.40	182.60	1320.00	169.69
z-axis	Frequency (Hz)	Stiffness (kN/m)	Damping (Kg/s)	Frequency (Hz)	Stiffness (kN/m)	Damping (Kg/s)	Frequency (Hz)	Stiffness (kN/m)	Damping (Kg/s)
HS	27.42	30.30	49.47	43.24	74.15	36.71	159.43	1040.00	359.53
HA	85.89	297.64	160.04	115.72	540.62	218.88	191.20	1450.00	184.75
HB	17.60	13.89	81.56	107.93	474.48	241.35	197.13	1540.00	184.21
HC	46.69	86.37	34.17	96.31	368.90	104.51	194.60	1500.00	166.23
HD	13.31	07.02	9.89	63.36	159.55	65.25	186.01	1380.00	193.26